BNL-105410-2014-TECH
EIC/43;BNL-105410-2014-IR

The influence of longitudinal space charge fields on the modulation process of coherent electron cooling

G. Wang

May 2014

Collider Accelerator Department
Brookhaven National Laboratory

U.S. Department of Energy
USDOE Office of Science (SC)

Notice: This technical note has been authored by employees of Brookhaven Science Associates, LLC under Contract No.DE-AC02-98CH10886 with the U.S. Department of Energy. The publisher by accepting the technical note for publication acknowledges that the United States Government retains a non-exclusive, paid-up, irrevocable, world-wide license to publish or reproduce the published form of this technical note, or allow others to do so, for United States Government purposes.

DISCLAIMER

This report was prepared as an account of work sponsored by an agency of the United States Government. Neither the United States Government nor any agency thereof, nor any of their employees, nor any of their contractors, subcontractors, or their employees, makes any warranty, express or implied, or assumes any legal liability or responsibility for the accuracy, completeness, or any third party's use or the results of such use of any information, apparatus, product, or process disclosed, or represents that its use would not infringe privately owned rights. Reference herein to any specific commercial product, process, or service by trade name, trademark, manufacturer, or otherwise, does not necessarily constitute or imply its endorsement, recommendation, or favoring by the United States Government or any agency thereof or its contractors or subcontractors. The views and opinions of authors expressed herein do not necessarily state or reflect those of the United States Government or any agency thereof.

BNL-105410-2014-IR

C-A/AP/513
May 2014

The influence of longitudinal space charge fields on the modulation process of coherent electron cooling

G. Wang, M. Blaskiewicz,
V.N. Litvinenko

Collider-Accelerator Department
Brookhaven National Laboratory
Upton, NY 11973

Notice: This document has been authorized by employees of Brookhaven Science Associates, LLC under Contract No. DE-AC02-98CH10886 with the U.S. Department of Energy. The United States Government retains a non-exclusive, paid-up, irrevocable, world-wide license to publish or reproduce the published form of this document, or allow others to do so, for United States Government purposes.

The Influence of Longitudinal Space Charge Fields on the Modulation Process of Coherent Electron Cooling

G. Wang, M. Blaskiewicz, V. N. Litvinenko

Abstract

Initial modulation in Coherent electron cooling (CeC) scheme relies on ion charge screening by electrons. In a CeC system with bunched electron beam, the long-range longitudinal space charge force is inevitably induced. For a relatively dense electron beam, it can be comparable or even greater than the attractive force from the ion. Hence, space-charge field influence to the modulation process could be important. If the longitudinal Debye length is much smaller than the electron bunch length, the modulation induced by the ion happens locally. In this case, the long-range longitudinal space charge field can be approximated as a uniform electric field across the region. In this paper we developed an analytical model to study the dynamics of ion shielding in the presence of a uniform electric field. We are solving the coupled Vlasov-Poisson equation system for infinite anisotropic electron plasma and estimate the influences of the longitudinal space charge field to the modulation process. We present numerical estimates for a case of the proof of CeC principle experiment at RHIC.

I. Introduction

Idea of Coherent electron Cooling (CeC) was first introduced by Y. Derbenev in 1980s [1]. In 2007, V. N. Litvinenko and Y. Derbenev have developed detailed theory of Free Electron Laser (FEL) based CeC scheme [2, 3]. It utilizes FEL as an amplifier and time-of-flight dependence on hadron's energy to cool hadrons. Estimations show that it has the potential to cool high-energy high-intensity ion beam in modern hadron accelerators such as RHIC, LHC and the proposed eRHIC. More recently, a similar CeC concept based on amplification via a micro-bunch instability, called by the author Micro-bunched Electron Cooling (MBEC), has been proposed [4]. The later technique has potential of much larger bandwidth compared with other CeC schemes [4]. A CeC system comprises of three sections: modulator, amplifier and kicker. In the modulator, the ion beam and the electron beam are merged together. Each ion creates an electron density modulation around itself through the process shielding, or screening. The electron density modulation is then amplified in the CeC amplifier and acts back on the ion in the kicker section. As the result, the energy error of the ion is reduced. By coupling transverse and longitudinal motions [2-3], the oscillations in all three degrees of freedom can be cooled.

The modulation process of CeC relies on the Coulomb interaction between electrons and ions. The dynamics of the process in uniform anisotropic electron plasma has been previously investigated, which, at the cold electron beam limit, reduces to the results obtained from the hydro-dynamical model [3, 5]. In these calculations, it is assumed that electrons have uniform spatial distribution and hence there is no net space charge field in the un-perturbed electron plasma. The assumption is valid if the spatial extension of the

electron bunch is much larger than the Debye lengths in all three dimensions and the ion is located close to the center of the electron bunch. However, for an electron bunch with high density and an ion interacting with electrons away from the bunch centers, the electrons surrounding the ion may see a net longitudinal space charge force comparable to or even greater than the attractive force from the ion. This makes it necessary to account for the long-range space charge field while analyzing the modulation process.

In this work, we withdraw the assumption that the net long-range space charge field is negligible while still assuming that the spatial distribution of electrons is smooth and its spatial extension is much larger than the Debye lengths in all three dimensions. With these assumptions, it is still possible to make the approximation that electrons participating in shielding a specific ion have uniform spatial distribution. Also, the long-range space charge field perceived by these electrons can be considered as uniform.

Consequently, the modulation process can be described by the self-consistent Vlasov-Poisson equation system for uniform electron plasma in the presence of a moving ion and an external electric field. By linearizing the Vlasov equation, we are able to solve the equation system for the κ-2 velocity distribution analytically and obtain the density modulation in a simple form of 1-D integral.

The paper is organized as follows. In section II, we write the linearized Vlasov-Poisson equation for the system and solve the equations for the background electrons. The linearized Vlasov-Poisson equation system is solved in section III, and the electron density modulation induced by the moving ion is obtained. In section IV we gives a few numerical examples for the influence of longitudinal long-range space charge field on the modulation process in the proof of principle experiment of CeC and the proposed CeC systems for eRHIC and LHC. The reduction of the longitudinal space charge field due to beam pipe screening is calculated in section V. Section VI presents the summary.

II. Linearized Vlasov-Poisson Equations

It is convenient to choose the reference frame as the rest frame of the ion, where the velocities of electrons are non-relativistic. Non-relativistic nature of the particles' motion in this frame allows us to use electrostatic Poisson equation as a good approximation for the evolution of electric fields.

Let $f(\vec{x},\vec{v},t)$ be the electron phase space density distribution at time t with the initial distribution at $t=0$ of:

$$f(\vec{x},\vec{v},0)=f_0(\vec{v}). \tag{1}$$

For $t>0$, the phase space distribution function is determined by the coupled Vlasov-Poisson equation system:

$$\frac{\partial}{\partial t}f(\vec{x},\vec{v},t)+\vec{v}\cdot\frac{\partial}{\partial \vec{x}}f(\vec{x},\vec{v},t)-\frac{e}{m_e}\left[\vec{E}_{ext}-\vec{\nabla}\phi_{ind}(\vec{x},t)\right]\cdot\frac{\partial}{\partial \vec{v}}f(\vec{x},\vec{v},t)=0\ , \tag{2}$$

and

$$\nabla^2\phi_{ind}(\vec{x},t)=-\frac{1}{\varepsilon_0}\left[Z_i e\delta(\vec{x})-e\int_{-\infty}^{\infty}f(\vec{x},\vec{v},t)d^3v\right], \quad (3)$$

where $\vec{E}_{ext}$ is the uniform space charge field at the location of the ion and $Z_i e$ is the electric charge of the ion. The electric potential, $\phi_{ind}(\vec{x},t)$, is induced both by the ion and the electrons' response to the ion's field. To linearize eq. (2), we write the phase space density as

$$f(\vec{x},\vec{v},t)=f_{BG}(\vec{x},\vec{v},t)+f_{ind}(\vec{x},\vec{v},t), \quad (4)$$

where the distribution function of background electrons, $f_{BG}(\vec{x},\vec{v},t)$, describes the evolution of the electron phase space density in the absence of the ion and satisfies

$$\frac{\partial}{\partial t}f_{BG}(\vec{x},\vec{v},t)+\vec{v}\cdot\frac{\partial}{\partial\vec{x}}f_{BG}(\vec{x},\vec{v},t)+\vec{a}\cdot\frac{\partial}{\partial\vec{v}}f_{BG}(\vec{x},\vec{v},t)=0, \quad (5)$$

with

$$\vec{a}\equiv-\frac{e}{m_e}\vec{E}_{ext}\ . \quad (6)$$

Since the acceleration does not depend either on the coordinate or on initial velocity, the evolution of the distribution is simply a shift of the initial distribution by $\Delta\vec{v}=\vec{a}t$:

$$f_{BG}(\vec{x},\vec{v},t)=f_0(\vec{v}-\vec{a}t). \quad (7)$$

Solution in eq. (7) explicitly satisfies eq. (5). Inserting eq. (4) into eq. (2) and making use of eq. (5) lead to the linearized Vlasov equation

$$\frac{\partial}{\partial t}f_{ind}(\vec{x},\vec{v},t)+\vec{v}\cdot\frac{\partial}{\partial\vec{x}}f_{ind}(\vec{x},\vec{v},t)+\vec{a}\cdot\frac{\partial}{\partial\vec{v}}f_{ind}(\vec{x},\vec{v},t)+\frac{e}{m_e}\vec{\nabla}\phi_{ind}(\vec{x},t)\cdot\frac{\partial}{\partial\vec{v}}f_0(\vec{v}-\vec{a}t)=0. \quad (8)$$

As the distribution of background electrons is uniform and hence does not contribute to the electric field, the electric potential, $\phi_{ind}(\vec{x},t)$, is solely determined by the electron density modulation:

$$\nabla^2\phi_{ind}(\vec{x},t)=-\frac{1}{\varepsilon_0}\left[Z_i e\delta(\vec{x})-e\int_{-\infty}^{\infty}f_{ind}(\vec{x},\vec{v},t)d^3v\right]. \quad (9)$$

Eqs. (8) and (9) constitute the linearized Vlasov-Poisson system, which determines the electron phase space density modulation induced by the ion.

III. Solving Linearized Vlasov-Poisson System for κ-2 Velocity Distribution

In order to proceed, it is convenient to change the independent variables, $\vec{v}$ and t, to a set of new variables:

$$\vec{u}\equiv\vec{v}-\vec{a}t\ , \quad (10)$$

and

$$\tau\equiv t\ .$$

We denote the induced phase space density variation in terms of the new variables as

$$f_1(\vec{x},\vec{u},\tau)\equiv f_{ind}(\vec{x},\vec{u}+\vec{a}\tau,\tau). \quad (11)$$

With the new variables, the partial derivatives in eq. (8) with respect to $\vec{v}$ and t can be rewritten as

$$\left.\frac{\partial}{\partial t} f_{ind}\left(\vec{x},\vec{v},t\right)\right|_{\vec{v}} = -\left.\frac{\partial}{\partial \vec{u}} f_1\left(\vec{x},\vec{u},\tau\right)\right|_{\tau} \cdot \vec{a} + \left.\frac{\partial}{\partial \tau} f_1\left(\vec{x},\vec{u},\tau\right)\right|_{\vec{u}}, \tag{12}$$

and

$$\vec{a} \cdot \left.\frac{\partial}{\partial \vec{v}} f_{ind}\left(\vec{x},\vec{v},t\right)\right|_{t} = \vec{a} \cdot \left.\frac{\partial}{\partial \vec{u}} f_1\left(\vec{x},\vec{u},\tau\right)\right|_{\tau}. \tag{13}$$

Inserting eqs. (12) and (13) into eq. (8) yields the linearized Vlasov equation in new variables:

$$\frac{\partial}{\partial \tau} f_1\left(\vec{x},\vec{u},\tau\right) + \left(\vec{u} + \vec{a}\tau\right) \cdot \frac{\partial}{\partial \vec{x}} f_1\left(\vec{x},\vec{u},\tau\right) + \frac{e}{m_e} \vec{\nabla} \phi_{ind}\left(\vec{x},\tau\right) \cdot \frac{\partial}{\partial \vec{u}} f_0\left(\vec{u}\right) = 0. \tag{14}$$

The Poisson equation, eq. (9), can be simply rewritten as

$$\nabla^2 \phi_{ind}\left(\vec{x},t\right) = -\frac{1}{\varepsilon_0}\left[Z_i e \delta\left(\vec{x}\right) - e \int_{-\infty}^{\infty} f_1\left(\vec{x},\vec{u},\tau\right) d^3u \right]. \tag{15}$$

Multiplying both sides of eqs. (14) and (15) by $e^{-i\vec{k}\cdot\vec{x}}$, and integrating over $\vec{x}$ gives their Fourier transformation:

$$\frac{\partial}{\partial \tau} \tilde{f}_1\left(\vec{k},\vec{u},\tau\right) + i\vec{k} \cdot \left(\vec{u} + \vec{a}\tau\right) \tilde{f}_1\left(\vec{k},\vec{u},\tau\right) = -i \frac{e}{m_e} \tilde{\phi}_{ind}\left(\vec{k},\tau\right) \vec{k} \cdot \frac{\partial}{\partial \vec{u}} f_0\left(\vec{u}\right), \tag{16}$$

and

$$\tilde{\phi}_{ind}\left(\vec{k},\tau\right) = \frac{e}{\varepsilon_0 k^2}\left[Z_i - \tilde{n}_1\left(\vec{k},\tau\right) \right]. \tag{17}$$

The Fourier components of the phase space density and electric potential are defined as:

$$\tilde{f}_1\left(\vec{k},\vec{u},\tau\right) = \int_{-\infty}^{\infty} f_1\left(\vec{x},\vec{u},\tau\right) e^{-i\vec{k}\cdot\vec{x}} d^3x, \tag{18}$$

$$\tilde{\phi}_{ind}\left(\vec{k},\tau\right) = \int_{-\infty}^{\infty} \phi_{ind}\left(\vec{x},\tau\right) e^{-i\vec{k}\cdot\vec{x}} d^3x, \tag{19}$$

and the Fourier components of the spatial density modulation is given by

$$\tilde{n}_1\left(\vec{k},\tau\right) = \int_{-\infty}^{\infty} \tilde{f}_1\left(\vec{k},\vec{u},\tau\right) d^3u. \tag{20}$$

Multiplying both sides of eq. (16) by $\exp\left(i\vec{k}\cdot\vec{u}\tau + i\vec{k}\cdot\vec{a}\frac{\tau^2}{2} \right)$ we can transform it into

$$\frac{\partial}{\partial\tau}\left[e^{i\vec{k}\cdot\left(\vec{u}+\frac{\vec{a}\tau}{2}\right)\tau}\tilde{f}_1\left(\vec{k},\vec{u},\tau\right)\right]=-i\frac{e}{m_e}\left[\vec{k}\cdot\frac{\partial}{\partial\vec{u}}f_0\left(\vec{u}\right)\right]e^{i\vec{k}\cdot\left(\vec{u}+\frac{\vec{a}\tau}{2}\right)\tau}\tilde{\phi}_{ind}\left(\vec{k},\tau\right), \tag{21}$$

which, after integration over τ, produces

$$\tilde{f}_1\left(\vec{k},\vec{u},\tau\right)=-i\frac{e}{m_e}\int_0^{\tau}\tilde{\phi}_{ind}\left(\vec{k},\tau_1\right)\mathrm{e}^{\frac{i\vec{k}\cdot\vec{a}\left(\tau_1^2-\tau^2\right)}{2}}\left[\vec{k}\cdot\frac{\partial}{\partial\vec{u}}f_0\left(\vec{u}\right)\right]\mathrm{e}^{i\vec{k}\cdot\vec{u}\left(\tau_1-\tau\right)}d\tau_1\ . \tag{22}$$

Inserting eq. (17) into (22) and then taking integration over $\vec{u}$ lead to the following integral equation

$$\tilde{n}_1\left(\vec{k},\tau\right)=\frac{e^2}{\varepsilon_0 m_e}\int_0^{\tau}d\tau_1\left[\tilde{n}_1\left(\vec{k},\tau_1\right)-Z_i\right]\mathrm{e}^{\frac{i\vec{k}\cdot\vec{a}\left(\tau_1^2-\tau^2\right)}{2}}\int_{-\infty}^{\infty}\left[\frac{i\vec{k}}{k^2}\cdot\frac{\partial}{\partial\vec{u}}f_0\left(\vec{u}\right)\right]\mathrm{e}^{i\vec{k}\cdot\vec{u}\left(\tau_1-\tau\right)}d^3u\ . \tag{23}$$

To move further, let's assume that the initial velocity distribution of electrons at $t=0$ is anisotropic κ-2 distribution, which in terms of the new variables reads:

$$f_0\left(\vec{u}\right)=\frac{n_0}{\pi^2\beta_x\beta_y\beta_z}\left[1+\frac{\left(u_x+v_{0x}\right)^2}{\beta_x^2}+\frac{\left(u_y+v_{0y}\right)^2}{\beta_y^2}+\frac{\left(u_z+v_{0z}\right)^2}{\beta_z^2}\right]^{-2}, \tag{24}$$

where $\vec{v}_0$ is the velocity of the ion and n_0 is the spatial density of the background electrons. Parameters β_x, β_y and β_z describe velocity spreads of electrons in the corresponding directions. Inserting eq. (24) into (23) and applying the relation

$$i\int_{-\infty}^{\infty}e^{i\vec{k}\cdot\vec{u}\tau}\frac{\vec{k}}{k^2}\cdot\frac{\partial}{\partial\vec{u}}f_0\left(\vec{u}\right)d^3u=\int_{-\infty}^{\infty}f_0\left(\vec{u}\right)e^{i\vec{k}\cdot\vec{u}\tau}\tau d^3u\ , \tag{25}$$

the integral equation reduces to

$$\begin{aligned}\tilde{n}_1\left(\vec{k},\tau\right)&=\omega_p^2\int_0^{\tau}\left[\tilde{n}_1\left(\vec{k},\tau_1\right)-Z_i\right]\mathrm{e}^{\frac{i\vec{k}\cdot\vec{a}\left(\tau_1^2-\tau^2\right)}{2}}\left(\tau_1-\tau\right)g\left(\vec{k}\left(\tau-\tau_1\right)\right)d\tau_1\\&=\omega_p^2\int_0^{\tau}\left[\tilde{n}_1\left(\vec{k},\tau_1\right)-Z_i\right]\mathrm{e}^{\frac{i\vec{k}\cdot\vec{a}\left(\tau_1^2-\tau^2\right)}{2}}\left(\tau_1-\tau\right)\mathrm{e}^{\lambda\left(\vec{k}\right)\left(\tau-\tau_1\right)}d\tau_1\end{aligned}, \tag{26}$$

where

$$g\left(\vec{q}\right)\equiv\frac{1}{n_0}\int_{-\infty}^{\infty}f_0\left(\vec{u}\right)e^{-i\vec{q}\cdot\vec{u}}d^3u=\exp\left[i\vec{q}\cdot\vec{v}_0-\sqrt{q_x^2\beta_x^2+q_y^2\beta_y^2+q_z^2\beta_z^2}\right], \tag{27}$$

$$\lambda\left(\vec{k}\right)\equiv i\vec{k}\cdot\vec{v}_0-\sqrt{k_x^2\beta_x^2+k_y^2\beta_y^2+k_z^2\beta_z^2}\ , \tag{28}$$

and

$$\omega_p \equiv \sqrt{\frac{n_0 e^2}{m_e \varepsilon_0}} \ . \tag{29}$$

Eq. (26) can be written into a more compact form:

$$\tilde{H}_1\left(\vec{k},\tau\right) = \omega_p^2 \int_0^\tau \left[\tilde{H}_1\left(\vec{k},\tau_1\right) - Z_i \mathrm{e}^{\frac{i\vec{k}\cdot\vec{a}\tau_1^2}{2} - \lambda\left(\vec{k}\right)\tau_1} \right] \left(\tau_1 - \tau\right) d\tau_1 \ , \tag{30}$$

and the new function, $\tilde{H}_1\left(\vec{k},\tau\right)$, is defined as

$$\tilde{H}_1\left(\vec{k},\tau\right) \equiv \tilde{n}_1\left(\vec{k},\tau\right) \mathrm{e}^{-\lambda\left(\vec{k}\right)\tau + \frac{i\vec{k}\cdot\vec{a}\tau^2}{2}} \ . \tag{31}$$

Taking the second time derivative of eq. (30) generates an inhomogeneous second-order ordinary differential equation (ODE)

$$\frac{d^2}{d\tau^2}\tilde{H}_1\left(\vec{k},\tau\right) + \omega_p^2 \tilde{H}_1\left(\vec{k},\tau\right) = Z_i \omega_p^2 \mathrm{e}^{\frac{i\vec{k}\cdot\vec{a}\tau^2}{2} - \lambda\left(\vec{k}\right)\tau} \ , \tag{32}$$

which, for arbitrary initial conditions, has the solution[6]

$$\tilde{H}_1\left(\vec{k},\tau\right) = c_1 \cos\left(\omega_p \tau\right) + c_2 \sin\left(\omega_p \tau\right) + Z_i \omega_p \int_0^\tau \sin\left[\omega_p\left(\tau - \tau_1\right)\right] \mathrm{e}^{\frac{i\vec{k}\cdot\vec{a}\tau_1^2}{2} - \lambda\left(\vec{k}\right)\tau_1} d\tau_1 \ , \tag{33}$$

with c_1 and c_2 being constants to be determined by the initial conditions at $t = 0$. As we assume that there is no modulation at $t = 0$, the initial conditions read

$$\tilde{H}_1\left(\vec{k},0\right) = \tilde{n}_1\left(\vec{k},0\right) = 0 \ , \tag{34}$$

and

$$\frac{d}{d\tau}\tilde{H}_1\left(\vec{k},\tau\right)\Big|_{\tau=0} = \frac{d}{d\tau}\tilde{n}_1\left(\vec{k},\tau\right)\Big|_{\tau=0} - \lambda\left(\vec{k}\right)\tilde{n}_1\left(\vec{k},0\right) = 0. \tag{35}$$

Applying the initial conditions of eq. (34) to eq. (33) for $\tau = 0$ yields

$$c_1 = 0 \, . \tag{36}$$

Inserting eq. (36) into (33) and then taking the first time derivative produces

$$\begin{aligned} \frac{d}{d\tau}\tilde{H}_1\left(\vec{k},\tau\right) = c_2 \omega_p \cos\left(\omega_p \tau\right) + Z_i \omega_p^2 \cos\left(\omega_p \tau\right) \int_0^\tau \cos\left(\omega_p \tau_1\right) \mathrm{e}^{\frac{i\vec{k}\cdot\vec{a}\tau_1^2}{2} - \lambda\left(\vec{k}\right)\tau_1} d\tau_1 \\ + Z_i \omega_p^2 \sin\left(\omega_p \tau\right) \int_0^\tau \sin\left(\omega_p \tau_1\right) \mathrm{e}^{\frac{i\vec{k}\cdot\vec{a}\tau_1^2}{2} - \lambda\left(\vec{k}\right)\tau_1} d\tau_1 \end{aligned} \ . \tag{37}$$

Eqs. (35) and (37) require

$$c_2 = 0 \, , \tag{38}$$

and hence we obtain from eqs. (33), (36) and (38)

$$\tilde{H}_1\left(\vec{k},\tau\right)=Z_i\omega_p\int_0^{\tau}\sin\left[\omega_p\left(\tau-\tau_1\right)\right]\mathrm{e}^{-\lambda\left(\vec{k}\right)\tau_1+\frac{i\vec{k}\cdot\vec{a}\tau_1^2}{2}}d\tau_1\ . \tag{39}$$

Substituting the definition of $\tilde{H}_1\left(\vec{k},\tau\right)$, eq. (31), back into eq. (39), we obtain the electron density modulation in the wave-vector domain

$$\tilde{n}_1\left(\vec{k},\tau\right)=Z_i\omega_p\int_0^{\tau}\sin\left[\omega_p\left(\tau-\tau_1\right)\right]\mathrm{e}^{\lambda\left(\vec{k}\right)\left(\tau-\tau_1\right)-\frac{i\vec{k}\cdot\vec{a}\left(\tau^2-\tau_1^2\right)}{2}}d\tau_1\,. \tag{40}$$

The electron density modulation in the configuration space is given by the inverse Fourier transformation of $\tilde{n}_1\left(\vec{k},\tau\right)$, i.e.

$$n_1\left(\vec{x},t\right)=\frac{1}{\left(2\pi\right)^3}\int_{-\infty}^{\infty}\tilde{n}_1\left(\vec{k},t\right)e^{i\vec{k}\cdot\vec{x}}d^3k\ . \tag{41}$$

Inserting eq. (40) into (41), we finally obtain the following expression for the electron density modulation induced by an ion

$$\begin{aligned}n_1\left(\vec{x},t\right)=\frac{Z_i}{\pi^2r_xr_yr_z}\int_0^{\omega_pt}\psi\sin\psi\Bigg[&\psi^2+\left(\overline{x}-\overline{a}_x\psi\left(\omega_pt-\frac{\psi}{2}\right)+\overline{v}_{0,x}\psi\right)^2\\&+\left(\overline{y}-\overline{a}_y\psi\left(\omega_pt-\frac{\psi}{2}\right)+\overline{v}_{0,y}\psi\right)^2+\left(\overline{z}-\overline{a}_z\psi\left(\omega_pt-\frac{\psi}{2}\right)+\overline{v}_{0,z}\psi\right)^2\Bigg]^{-2}d\psi\end{aligned}\ , \tag{42}$$

where we have used the normalized variables defined as $\overline{x}_j\equiv x_j/r_j$, $\overline{a}_j\equiv a_j/r_j\omega_p^2$, $\overline{v}_{0,j}=v_{0,j}/\beta_j$ and $r_j\equiv\beta_j/\omega_p$ for $j=x,y,z$. Eq. (42) has the form of a 1-D integral with finite integration range and as expected, it reduces to the previously derived results at the limit of $\vec{a}=0$. Fig. 1 and Fig. 2 show the 1-D and 2-D plots of the electron density modulation obtained by numerical integration of eq. (42). In Fig. 1, the electron density modulations at a specific transverse location are plotted for various longitudinal space charge fields. For an ion at rest, as seen in Fig. 1(a) and Fig. 2(a), the space charge field reduces the peak modulation amplitude and shifts its longitudinal location. For a moving ion, however, Fig. 1(b) and Fig. 2(b) show that the acceleration of electrons due to space charge field can compensate the effects due to ion motion if the space charge force is in the same direction of the ion velocity. Qualitatively this can be understood as matching between the hadron velocity and average velocity of the electrons during the interaction process. Hence, matching average electron's velocity with that of the ion should increase the amplitude of modulation. Direct numerical evaluation of eq. (42) shown that the effect is nearly compensated (within a few percent deviation) when normalized velocity and the acceleration is matched. Fig. 3 illustrates such compensation for three phase advances of the plasma oscillations. The matching naturally depends on the phase advance. At phase advance $\omega_pt=\pi/4$, the matching occurs at about $\overline{v}_z\approx0.63\overline{a}_z$. For phase advances of $\omega_pt=\pi/2$ and $\omega_pt=\pi$ the matching ratios are $\overline{v}_z\approx1.35\overline{a}_z$

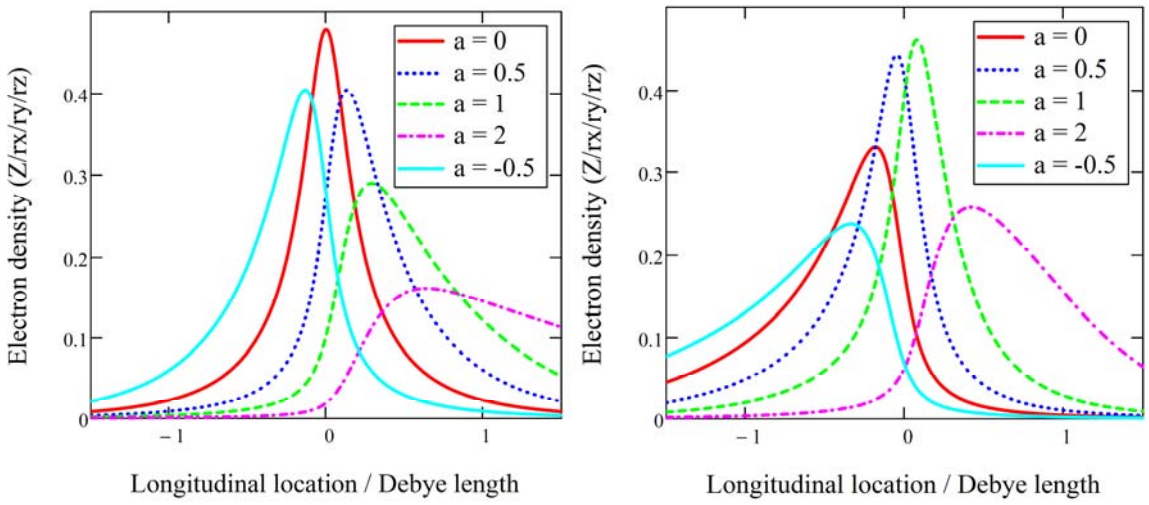

(a) (b)

Figure 1. Profiles of the density modulation induced by an ion in the presence of an external electric field (as calculated in eq. (42)). The external electric field is along z direction and the following values are used for the normalized acceleration, $\bar{a}_z$: 0 (red), 0.5 (blue), 1 (green), 2 (magenta), and -0.5 (light blue). The abscissa is the longitudinal location in units of longitudinal Debye length, r_z, and the ordinate is the electron density at transverse location $x = 0.1r_x$ and $y = 0.1r_y$ in units of $Z_i / \left(r_x r_y r_z\right)$. The snapshot is taken at $\omega_p t = \pi / 2$. (a) the ion is at rest; (b) the ion is moving with velocity $v_{0,z} = \beta_z$.

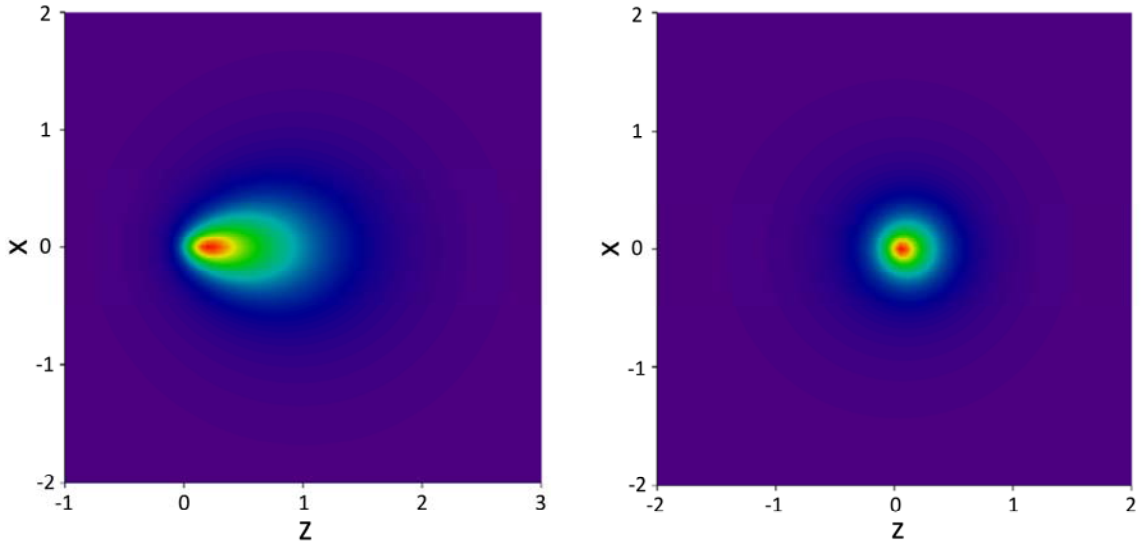

(a) (b)

Figure 2. Electron density modulation induced by an ion in the presence of an external electric field in the z direction with $\bar{a}_z = 1$. The abscissa is the location along z direction in units of the longitudinal Debye length, r_z, and the ordinate is the location along x in units of Horizontal Debye length, r_x. (a) the ion is at rest; (b) the ion is moving at $v_{0,z} = \beta_z$. The snapshot is taken at $\omega_p t = \pi / 2$ and $y = 0.1r_y$.

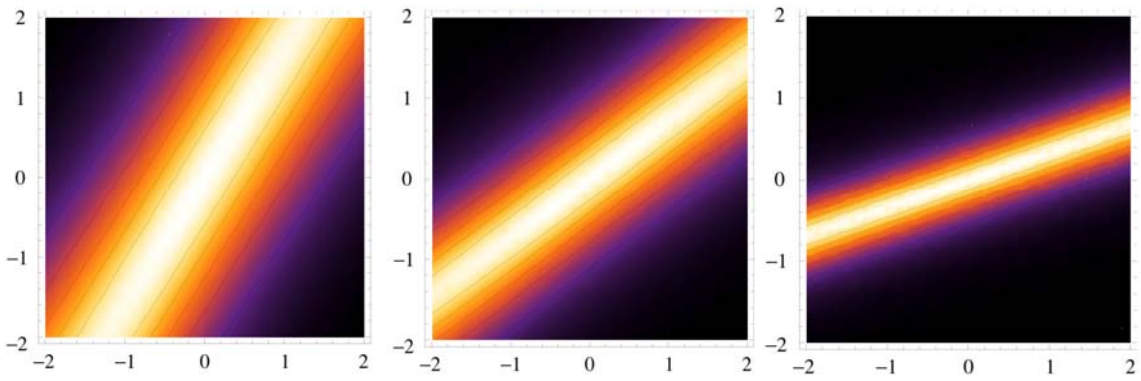

(a) (b) (c)

Figure 3. Plots of the normalized density at $z = 0$, $x = 0.1r_x$ and $y = 0.1r_y$ as functions of $\bar{v}_z$ (horizontal axis) and $\bar{a}_z$ (vertical axis) for three phase advances of plasma oscillations: (a) $\omega_p t = \pi/4$; (b) $\omega_p t = \pi/2$, and (c) $\omega_p t = \pi$. The distributions are normalized to their maximum values and the contour lines are spaced by 0.2.

and $\bar{v}_z \approx 2.9\bar{a}_z$, correspondingly.

As FEL only amplifies electron current modulation with frequencies close to its resonant frequency, the following quantity is closely related to the modulation efficiency:

$$\eta(k_z,t) \equiv \int_{-\infty}^{\infty} dz e^{-ik_z z} \int_{-\infty}^{\infty} n_1(x,y,z,t)\,dx\,dy. \tag{43}$$

Inserting eq. (41) into (43) leads to

$$\begin{aligned} \eta(k_z,t) &= \frac{1}{2\pi}\int_{-\infty}^{\infty} dk_{1,z}\tilde{n}_1(0,0,k_{1,z},t)\int_{-\infty}^{\infty} e^{i(k_{1,z}-k_z)z}\,dz \\ &= \tilde{n}_1(0,0,k_z,t) \end{aligned} \tag{44}$$

Making use of eq. (40), eq. (44) becomes

$$\eta(k_z,t) = Z_i \int_0^{\omega_p t} \exp\left[-i\bar{k}_z\bar{a}_z\psi\left(\omega_p t - \frac{\psi}{2}\right) + \left(i\bar{k}_z\cdot\bar{v}_{0,z} - \left|\bar{k}_z\right|\right)\psi\right]\sin\psi\,d\psi\ . \tag{45}$$

Fig. 4 plot the amplitude and phase of $\eta(k_z,t)$ for various acceleration parameters as a function of $k_z r_z$. As shown in Fig. 4(a), for $|a_z| \le r_z\omega_p^2$ and the FEL resonant wavelength $\lambda_{FEL} \ge 2\pi r_x$, the amplitude change due to longitudinal space charge is negligible. However, Fig. 4(b) shows that considerable phase shift can occur even for modest acceleration due to space charge field. To qualitatively understand the impact of longitudinal space charge field to CeC modulation process, as examples, we shall continue with numerical calculations for a few proposed CeC schemes.

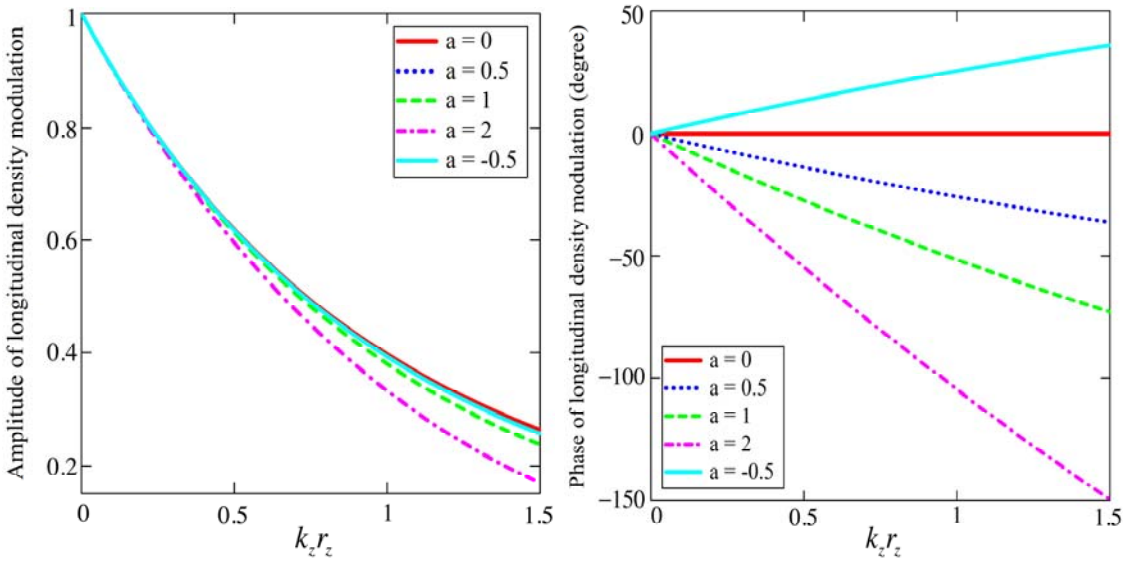

(a) (b)

Figure 4: Fourier components of the longitudinal density modulation as calculated from eq. (45) for various normalized acceleration parameters. The abscissa is the normalized longitudinal wave number, $k_z r_z$ and the plots are taken at $\omega_p t = \pi/2$. (a) the ordinate is $\left|\eta\left(k_z,t\right)\right|/Z_i$; (b) the ordinate is the phase shift of $\eta\left(k_z,t\right)$ with respect to that of zero acceleration parameter.

IV. Numerical Examples

The CeC proof of principle (CeC PoP) experiment is under construction at BNL [7] and a few possible CeC designs has been proposed [8]. The designed electron beam parameters for three CeCs are listed in Table 1 [7, 8]. In this section we estimate the effects of the longitudinal long-range space charge field on the modulation process for these parameters.

Table 1: Electron beam parameters for the Proof of Principle Experiment of CeC

Parameter/CeC	CeC PoP	eRHIC CEC	LHC CeC
Bunch charge, nC	1	10	30
Bunch length, rms, beam frame, σ_z , m	0.126	6.3	893
Beam radius R, mm	1.3	0.35	0.15
R/ σ_z	$1.03\cdot10^{-2}$	$5.56\cdot10^{-5}$	$1.68\cdot10^{-7}$
Energy (MeV)/ γ	21.5 / 42	136.2 / 266	3,812 / 7,460
Longitudinal Debye length at the bunch center, beam frame, μm	42	19.1	21.7
Plasma phase advance in modulator, rad	$\pi/2$	$\pi/2$	0.062

It is well known, that space charge effects fall very fast with the energy of the particles. Hence, we shall first consider the space charge effects for the CeC PoP experiment and later make relevant estimates for two other cases.

We shall, first, calculate the longitudinal space charge field inside the electron bunch. For simplicity, we only calculate the longitudinal space charge field at the bunch axis, i.e. for $x = y = 0$. In addition, we also assume the electron bunch has beer-can transverse distribution, i.e. the electron density is uniform for $r \le R$ and zero for $r > R$. The system has cylindrical symmetry and hence it is more convenient to use cylindrical coordinates. As illustrated in Fig. 5, the longitudinal space charge field at location $(0,0,l)$ contributed by electrons in an infinitesimal volume at location (r,φ,ζ) is given by[1]

$$\Delta E_z(l;r,\theta,\zeta) = \frac{r(l-\zeta)\rho(\zeta)\theta(R-r)\Delta\zeta\Delta r\Delta\varphi}{4\pi\varepsilon_0\left[(\zeta-l)^2+r^2\right]^{\frac{3}{2}}}, \tag{46}$$

where $\theta(x)$ is the Heaviside step function with the definition

$$\theta(x) \equiv \begin{cases} 1, & x \ge 0 \\ 0, & x < 0 \end{cases}, \tag{47}$$

and $\rho(\zeta)$ is the electron charge density in the beam frame for $r \le R$. Integrating eq. (46) over the transverse beam area yields the space charge field at location $(0,0,l)$ due to a longitudinal slice of electrons at longitudinal location ζ with width $\Delta\zeta$

$$\Delta E_z(l;\zeta) = \frac{\rho(\zeta)\Delta\zeta}{2\varepsilon_0}\left[\frac{l-\zeta}{|l-\zeta|} - \frac{l-\zeta}{\sqrt{(l-\zeta)^2+R^2}}\right]. \tag{48}$$

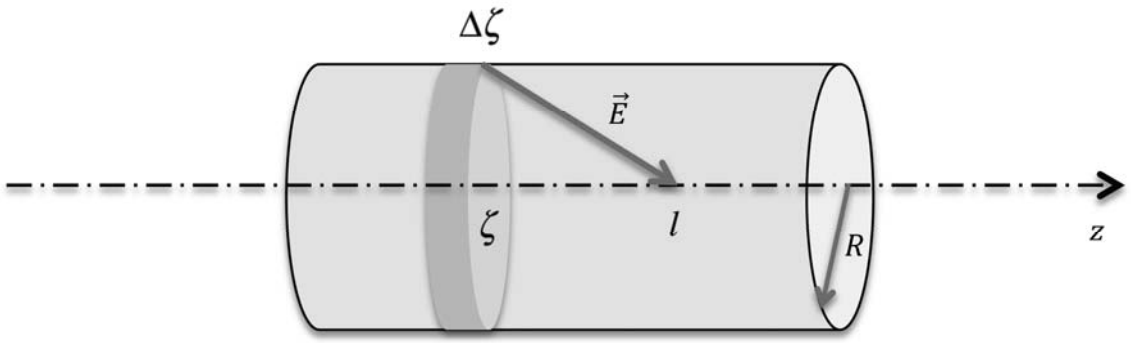

Figure 5. Illustration of the longitudinal space charge field calculation.

[1] In this section, we use notation l to represent the global longitudinal location along the bunch where space charge varies substantially, while leaving z for the local longitudinal coordinate where the characteristic scale is the longitudinal Debye length and the variation of space charge field is negligible.

To proceed, we assume the electron charge distribution at $r \le R$ has the following form

$$\rho(\zeta) = \frac{Q_e}{\pi R^2} \frac{1}{\sqrt{2\pi}\sigma_z} e^{-\frac{\zeta^2}{2\sigma_z^2}}, \tag{49}$$

where Q_e is the total charge of the electron bunch and σ_z is the R.M.S. electron bunch length. Inserting eq. (49) into (48) and then integrating over z yields the longitudinal space charge field at the location $(0,0,z_0)$

$$E_z(l) = \frac{-Q_e}{\sqrt{2}\pi^{\frac{3}{2}}\varepsilon_0\sigma_z^2} \cdot F\left(\frac{l}{\sigma_z}, \frac{R}{\sigma_z}\right), \tag{50}$$

with

$$F(\zeta,\chi) \equiv \frac{e^{-\frac{\zeta^2}{2}}}{\chi^2} \cdot \int_0^\infty e^{-\frac{\xi^2}{2}} \sinh(\zeta\cdot\xi)\left(\frac{\xi}{\sqrt{\xi^2+\chi^2}} - 1\right) d\xi. \tag{51}$$

It is worth nothing that, as shown in Fig. 6, even though the values of R/σ_z varies by five orders of magnitudes for the three cases listed in table 1, the peak values of $F(l/\sigma_z, R/\sigma_z)$ only changes by a factor of four. Eq. (50) is numerically evaluated for the CeC PoP parameters and the results are plotted in Fig. 10 (blue), which shows the maximal longitudinal space charge field reaches about 1.5 KV/m.

As shown in the previous section, the effects of the space charge relate to the normalized acceleration parameter, $\bar{a}_z$, which can be calculated as follows:

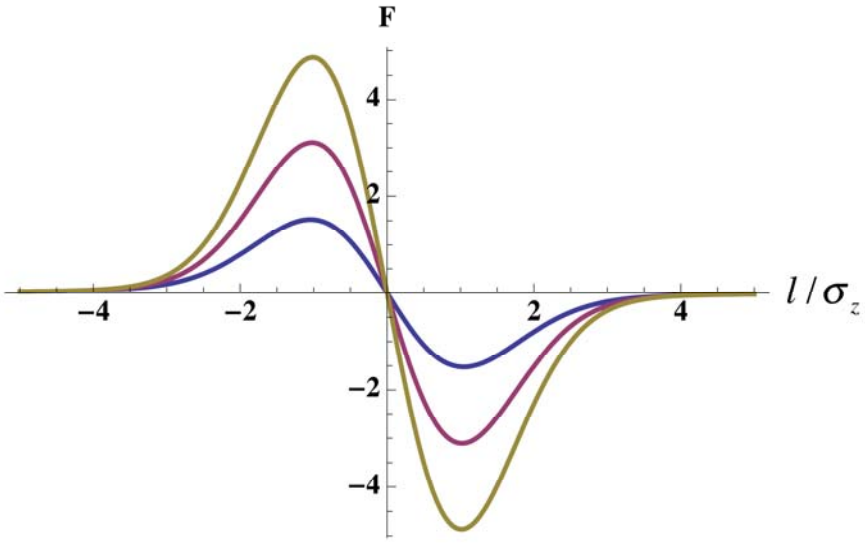

Figure 6. Plot of the F function for three R/σ_z parameters in Table 1 vs l/σ_z. Blue is for the CeC PoP case, magenta is for eRHIC CeC and grey-green is for LHC CeC.

$$\bar{a}_z(l) = \frac{-eE_z(l)}{m_e \beta_z \omega_p(l)} = \frac{-eE_z(l)}{m_e r_z(0) \omega^2{}_p(0)} \cdot e^{\frac{l^2}{4\sigma_z^2}}, \tag{52}$$

where

$$\omega_p(0) = \sqrt{\frac{|Q_e| e}{\sqrt{2\pi^3} R^2 \sigma_z m_e \varepsilon_0}}, \tag{53}$$

and

$$r_z(0) = \frac{\beta_z}{\omega_p(0)} \tag{54}$$

are the plasma frequency and the longitudinal Debye length at the electron bunch center. The plasma frequency at location l is

$$\omega_p(l) = e^{-\frac{l^2}{4\sigma_z^2}} \omega_p(0) \quad . \tag{55}$$

Making use of eqs. (50) and (48), we obtain the expression for the normalized acceleration parameter as follows

$$\bar{a}_z(l) = \frac{R^2}{r_z(0) \cdot \sigma_z} e^{\frac{l^2}{4\sigma_z^2}} \cdot F\left(\frac{l}{\sigma_z}, \frac{R}{\sigma_z}\right), \tag{56}$$

Fig. 7 plots the normalized acceleration parameter along the electron bunch for the CeC PoP parameters, suggesting that the normalized acceleration parameter stays below one within $\pm 4\sigma_z$ of the bunch.

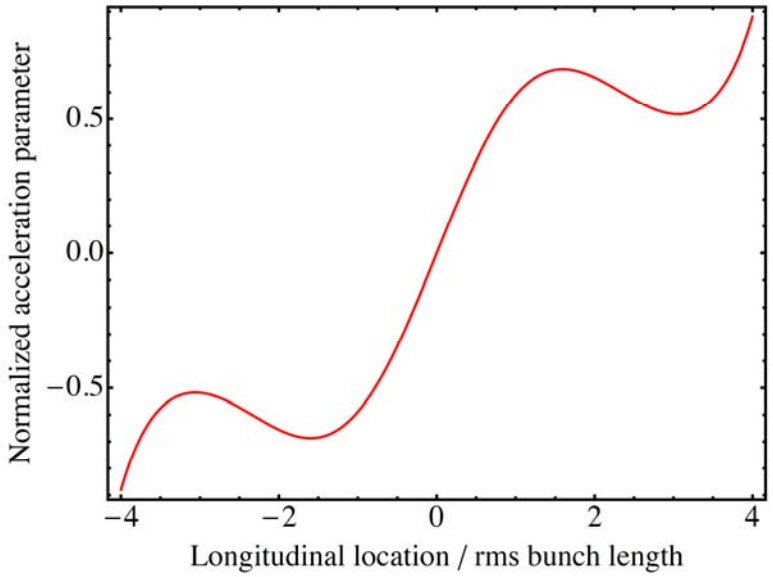

Figure 7: Normalized acceleration parameter due to space charge field (for the CeC PoP parameters listed in Table 1) as function of the longitudinal coordinate within a bunch.

The apparent growth of $|\bar{a}_z(l)|$ at $|l|/\sigma_z > 3$ in Fig. 7 does not mean that the effects of space charge field on the modulation are stronger for electrons far away from the bunch center. Since in practice, the time of interaction $t = \varphi_p(0)/\omega_p(0)$ is fixed, not the local phase advances of plasma oscillations $\varphi_p(l) = \omega_p(l)t$ with l being the distance from the bunch center. Hence, for the proper evaluation of the space charge effect at $l \neq 0$, one should evaluate eq. (42) at

$$\omega_p(l)t = \varphi_p(0)\exp(-l^2/4\sigma_l^2). \quad (57)$$

Fig. 8 illustrates the dependence the density modulation on $\bar{a}_z$ as function of the phase of plasma oscillation, e.g. eq.(57). It can be easily seen that at small phase advances, the dependence is very weak. One can see from Fig. 7 that $\bar{a}_z$ reaches a local extreme of $|\bar{a}_z| \sim 0.7$ at $|z|/\sigma_z \approx 1.75$. At this location plasma frequency is twice smaller that in the beam center, and with $\varphi_p(0) = \pi/2 \rightarrow \varphi_p(1.75) \propto \pi/4$. Hence, the effect on the peak density does not exceed 10 percent for $|\bar{a}_z| \sim 0.7$. In addition, at $|z|/\sigma_z \approx 1.75$ the e-beam peak current is about 1/5th of that in the center. Therefore, the FEL-based CeC, the FEL gain is turned off at this location and this part of the beam, naturally, does not effectively participate in the cooling process.

To account for the variation of $\omega_p(l)$ along the bunch while estimating the influences of longitudinal space charge field on modulation efficiency, we rewrite eq. (45) into the un-normalized variables:

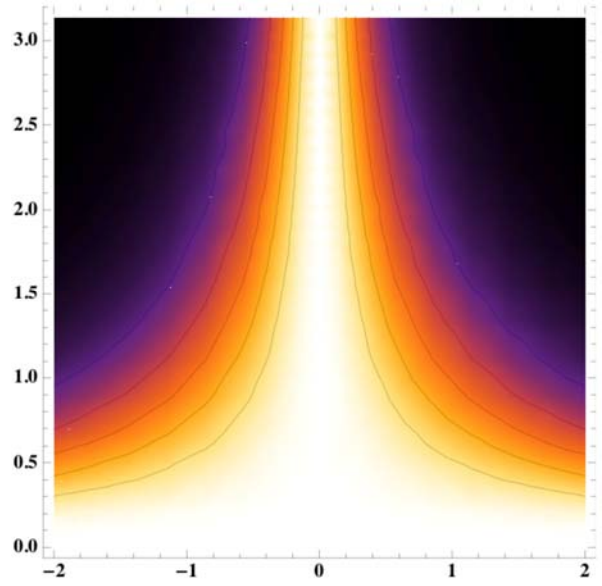

Figure 8. Plots of the normalized density at $z = 0$, $x = 0.1r_x$ and $y = 0.1r_y$ as functions of $\bar{a}_z$ (horizontal axis) and $\varphi_p = \omega_p t$ (vertical axis) $\omega_p t = \pi$. The distributions are normalized to their values at $\bar{a}_z = 0$. The contour lines are spaced by 0.2.

$$\eta\left(k_z,t,l\right)=Z_i\omega_p\left(l\right)\int_0^t\exp\left[-ik_z a_z\left(l\right)\left(t-\frac{\tau}{2}\right)\tau+\left(ik_z\cdot v_{0,z}-\left|k_z\right|\beta_z\right)\tau\right]\sin\left(\omega_p\left(l\right)t\right)d\tau, \tag{58}$$

and the space charge influences along the electron bunch can be represented by the following quantities:

$$\Delta\eta_{amp}\left(k_z,t,l\right)\equiv\frac{\left|\eta\left(k_z,t,l\right)\right|-\left|\eta_0\left(k_z,t,l\right)\right|}{\left|\eta_0\left(k_z,t,l\right)\right|}, \tag{59}$$

and

$$\Delta\eta_{ph}\left(k_z,t,l\right)\equiv\arg\left[\eta\left(k_z,t,l\right)\right]-\arg\left[\eta_0\left(k_z,t,l\right)\right], \tag{60}$$

where

$$\eta_0\left(k_z,t,l\right)=Z_i\omega_p\left(l\right)\int_0^t\exp\left[\left(ik_z\cdot v_{0,z}-\left|k_z\right|\beta_z\right)\tau\right]\sin\left(\omega_p\left(l\right)t\right)d\tau \tag{61}$$

is Fourier components in the absence of the space charge effects, i.e. $a_z=0$. Fig. 9 plots the relative changes of $\eta\left(k_z,t,l\right)$ as calculated from eqs. (59) and (60) for the proof of CeC principle experiment.

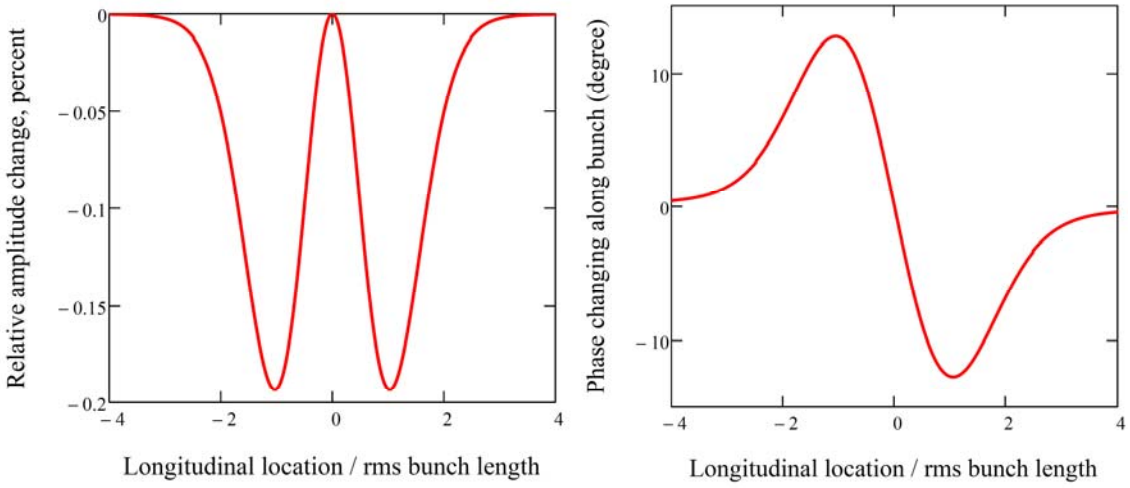

(a) (b)

Figure 9: influences of the longitudinal space charge field on the Fourier components of the longitudinal density modulation at the FEL resonant wavelength as a function of longitudinal location along the electron bunch. The ion is at rest and parameters from the proof of CeC principle experiment are applied in generating these plots. The abscissa is the longitudinal location in unit of R.M.S. bunch length. (a) the relative change of Fourier component amplitude in percentage as calculated from eq. (59); (b) the phase change of Fourier component in degree as calculated from eq. (60).

As shown in Fig. 9(a), the amplitude reduction of the wave-packets due to longitudinal space charge effects at the modulator is below 0.2%. However, Fig. 9(b) shows that the phase change of the initial modulation will result in the maximal wave-packet phase shift of ± 13 degrees. Since the reduction of the CeC efficiency is proportional to the cosine of phase shift, this effect would reduce CeC efficiency by less than 3%.

Compared with the CeC proof of principle experiment, the longitudinal space charge fields for the other two cases listed in the Table 1 are dramatically lower. In eRHIC CeC scheme, the space charge field strength peaks at 6.15 V/m, while for LHC CeC scheme, the space charge field is about 0.001 V/m. Consequently, the peak value of $\overline{a}_z$ reduces to $\pm\, 0.003$ and $\pm\, 3.7\times 10^{-6}$ respectively for the proposed eRHIC and LHC CeC schemes.

V. Screening effects from beam pipe

In reality, the electron bunch is usually enclosed by metallic vacuum chamber and the walls of vacuum chamber can reduce the strength of the longitudinal field induced by the space charge. For $\sigma_z / b >> 1$, the longitudinal space charge field in terms of the beam frame variables is given by [9]

$$E_{scr,z}(z) = -\frac{e}{4\pi\varepsilon_0}\left[2\ln\left(\frac{b}{R}\right)+1\right]\frac{d\lambda}{dz}, \tag{62}$$

where b is the beam pipe radius and

$$\lambda(z) = -\frac{\pi R^2}{e}\rho(z)\,, \tag{63}$$

is the electron line number density. Inserting eq. (49) into eq. (62) yields

$$E_{app,z}(z) = \frac{Q_e}{4\sqrt{2}\pi^{\frac{3}{2}}\varepsilon_0\sigma_z^2}\left[2\ln\left(\frac{b}{R}\right)+1\right]\frac{z}{\sigma_z}e^{-\frac{z^2}{2\sigma_z^2}}. \tag{64}$$

More generally, in the presence of a circular perfect conducting beam pipe, the on-axis longitudinal space charge field of an electron bunch with the distribution of eq. (49) and arbitrary bunch length is given by the following 1-D integral (Appendix A):

$$E_{exa,z}(0,z) = -\frac{Q_e}{\varepsilon_0\pi^2 R}\int_0^\infty e^{-\frac{k_z^2\sigma_z^2}{2}}\left[\frac{I_1(k_zR)K_0(k_zb)}{I_0(k_zb)}+K_1(k_zR)-\frac{1}{k_zR}\right]\sin(k_zz)\,dk_z\,, \tag{65}$$

where $I_n(x)$ and $K_n(x)$ are the modified Bessel functions. The space charge field calculated from eqs. (64) and (65) for the parameters of the proof of CeC principle experiment are plotted in Fig. 10, showing that the formulae agrees well for the considered parameters. More importantly, Fig. 10 suggests that the shielding effects from a perfectly conducting beam pipe wall reduce the peak longitudinal space charge field by 20%.

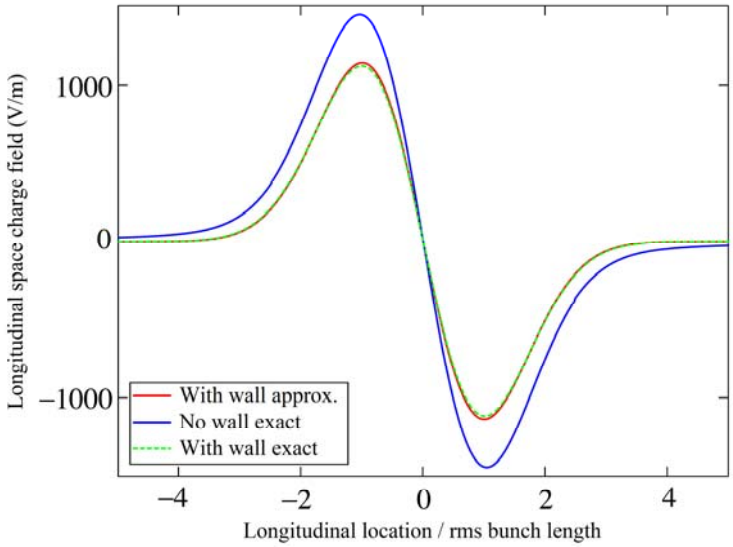

Figure 10. The longitudinal space charge field of an electron bunch in the free space (blue) and inside a beam pipe (red and green). The blue curve is generated using eq. (50) for an electron bunch in the free space, the red curve is produced by the approximate formula, eq. (64), for a long electron bunch inside a beam pipe, and the green curve is created from the exact formula, eq. (65), for an electron bunch with arbitrary bunch length inside a beam pipe. The proof of CeC principle experiment parameters are applied for all plots.

VI. Summary

In this work, we have developed an analytical model to study the ion shielding in the presence of a uniform electric field. The model assumes uniform electron spatial distribution and anisotropic 3-D velocity distribution. We shown that the electron density modulation induced by a moving ion can be expressed as a 1-D integral, which depends both on the ion velocity and the acceleration of electrons caused by the external field. Higher electron peak density modulation occurs when the acceleration of electrons is along the same direction of the ion velocity.

The model was applied to the process in the CeC modulator in the presence of space charge field. Its use is valid if the spatial extension of the electron bunch is much larger than the corresponding Debye length. As a numerical example, we estimated influence of the longitudinal space charge field on the modulation process in CeC used for the proof of principle experiment at BNL as well as for the proposed eRHIC and LHC CeC.

For the CeC PoP experiment, our estimations show that effect is relatively mild and can cause reduction of the CeC efficiency only by a few percent. More importantly, this analysis confirmed our early estimations and conclusions, that longitudinal space charge effects do not play significant role in the CeC schemes proposed for eRHIC and LHC.

References

[1] Y. S. Derbenev, in 7th All Union Conference on Charged Particle Accelerators Dubna, USSR, 1980.
[2] V. N. Litvinenko and Y. S. Derbenev, in 29th International Free Electron Laser Conference, Budker INP, Novosibirsk, Russia, 2007, p. 268.
[3] V. N. Litvinenko and Y. S. Derbenev, Physical Review Letters 102 (2009) 114801.
[4] D. Ratner, Physical Review Letters 111 (2013) 084802.
[5] G. Wang and M. Blaskiewicz, Phys. Rev. E 78 (2008) 026413.
[6] I. Gradshteyn and I. Ryzhik, Tables of Integrals, Series and Products, Academic Press, New York, 2007.
[7] I. Pinayev, et al., in the 4th International Particle Accelerator Conference, Shanghai, China, 2013, p. 1535.
[8] V. N. Litvinenko, in COOL 2013 workshop, Murren, Switzerland, 2013, p. 175.
[9] S.-Y. Lee, Accelerator physics, World Scientific, 2004.

Equation Chapter (Next) Section 1

Appendix A: Longitudinal space charge field of a charged bunch inside a conducting circular pipe:

For a charged particle bunch enclosed by an infinitely long conducting beam pipe with radius b, the electric potential, φ, at the beam pipe is equal to its value at infinity, which makes it possible to set the boundary condition as

$$\varphi(b,\theta,z)=\varphi(r,\theta,\infty)=0. \tag{A1}$$

We assume the charged particle bunch is transversely uniform with radius R and its total charge is Q_e. In the co-moving frame of the bunch, Poisson equation inside the beam pipe reads

$$\nabla^2\varphi=-\frac{Q_e}{\varepsilon_0\pi R^2}\frac{1}{\sqrt{2\pi}\sigma_z}e^{-\frac{z^2}{2\sigma_z^2}}\theta(R-r), \tag{A2}$$

where $\theta(x)$ is the Heaviside step function with the definition

$$\theta(x)\equiv\begin{cases}1, & x\geq 0\\ 0, & x<0\end{cases}. \tag{A3}$$

In cylindrical coordinates, eq. (A2) becomes

$$\frac{1}{r}\frac{\partial}{\partial r}\left(r\frac{\partial}{\partial r}\right)\varphi+\frac{1}{r^2}\frac{\partial^2}{\partial\theta^2}\varphi+\frac{\partial^2}{\partial z^2}\varphi=-\frac{Q_e}{\varepsilon_0\pi R^2}\frac{1}{\sqrt{2\pi}\sigma_z}e^{-\frac{z^2}{2\sigma_z^2}}\theta(R-r). \tag{A4}$$

Since the system has cylindrical symmetry, the derivative with respect to the azimuthal angle, θ, vanishes and hence eq. (A4) reduces to

$$\frac{1}{r}\frac{\partial}{\partial r}\left(r\frac{\partial}{\partial r}\right)\varphi+\frac{\partial^2}{\partial z^2}\varphi=-\frac{Q_e}{\varepsilon_0\pi R^2}\frac{1}{\sqrt{2\pi}\sigma_z}e^{-\frac{z^2}{2\sigma_z^2}}\theta(R-r)\ . \tag{A5}$$

Taking Fourier transformation of eq. (A5) along z axis yields:

$$\frac{1}{r}\frac{\partial}{\partial r}\left(r\frac{\partial}{\partial r}\right)\tilde{\varphi}_{in}(r,k_z)-k_z^2\tilde{\varphi}_{in}(r,k_z)=-\frac{Q_e}{\varepsilon_0\pi R^2}e^{-\frac{k_z^2\sigma_z^2}{2}}\theta(R-r)\ , \tag{A6}$$

where

$$\tilde{\varphi}(r,k_z)\equiv\int_{-\infty}^{\infty}e^{-ikz}\varphi(r,z)dz\ . \tag{A7}$$

The boundary condition for $\tilde{\varphi}(r,k_z)$ at $r=b$ is obtained from eq. (A1) and (A7) as

$$\tilde{\varphi}(b,k_z)=0. \tag{A8}$$

Expanding the first term of eq. (A6) yields

$$\frac{\partial^2}{\partial r^2}\tilde{\varphi}_{in}(r,k_z)+\frac{1}{r}\frac{\partial}{\partial r}\tilde{\varphi}_{in}(r,k_z)-k_z^2\tilde{\varphi}_{in}(r,k_z)=-\frac{Q_e}{\varepsilon_0\pi R^2}e^{-\frac{k_z^2\sigma_z^2}{2}}\theta(R-r). \tag{A9}$$

For $r\le R$, eq. (A9) can be rewritten into

$$\frac{\partial^2}{\partial\tilde{r}^2}\tilde{\varphi}_{in}(\tilde{r},k_z)+\frac{1}{\tilde{r}}\frac{\partial}{\partial\tilde{r}}\tilde{\varphi}_{in}(\tilde{r},k_z)-\tilde{\varphi}_{in}(\tilde{r},k_z)=-\frac{Q_e}{\varepsilon_0\pi k_z^2R^2}e^{-\frac{k_z^2\sigma_z^2}{2}}\ , \tag{A10}$$

with

$$\tilde{r}=k_zr\ . \tag{A11}$$

Eq. (A10) is the inhomogeneous modified Bessel differential equation and its solution can be expressed as

$$\tilde{\varphi}_{in}(\tilde{r},k_z)=\tilde{\varphi}_{in,h}(\tilde{r},k_z)+\tilde{\varphi}_{in,p}(\tilde{r},k_z), \tag{A12}$$

where

$$\tilde{\varphi}_{in,h}(\tilde{r},k_z)=c_1(k_z)I_0(\tilde{r})+c_2(k_z)K_0(\tilde{r}) \tag{A13}$$

is the solution of the homogeneous modified Bessel differential equation, i.e.

$$\frac{\partial^2}{\partial\tilde{r}^2}\tilde{\varphi}_{in,h}(\tilde{r},k_z)+\frac{1}{\tilde{r}}\frac{\partial}{\partial\tilde{r}}\tilde{\varphi}_{in,h}(\tilde{r},k_z)-\tilde{\varphi}_{in,h}(\tilde{r},k_z)=0\ , \tag{A14}$$

and $\tilde{\varphi}_{in,p}(k_z,\tilde{r})$ is the particular solution satisfying eq. (A10). Since the driving term in eq. (A10) is independent of $\tilde{r}$, the particular solution reads

$$\tilde{\varphi}_{in,p}(\tilde{r},k_z)=\frac{Q_e}{\varepsilon_0\pi k_z^2R^2}e^{-\frac{k_z^2\sigma_z^2}{2}}\ . \tag{A15}$$

Inserting eqs. (A13) and (A15) into eq. (A12) yields

$$\tilde{\varphi}_{in}(\tilde{r},k_z)=c_1(k_z)I_0(\tilde{r})+c_2(k_z)K_0(\tilde{r})+\frac{Q_e}{\varepsilon_0\pi k_z^2R^2}e^{-\frac{k_z^2\sigma_z^2}{2}}\ . \tag{A16}$$

Requiring $\tilde{\varphi}_{in}\left(\tilde{r}=0\right)$ being finite leads to

$$\tilde{\varphi}_{in}\left(\tilde{r},k_z\right)=c_1\left(k_z\right)I_0\left(\tilde{r}\right)+\frac{Q_e}{\varepsilon_0\pi k_z^2R^2}e^{-\frac{k_z^2\sigma_z^2}{2}}. \tag{A17}$$

For $r>R$, eq. (A9) becomes the homogeneous modified Bessel differential equation

$$\frac{\partial^2}{\partial\tilde{r}^2}\tilde{\varphi}_{out}\left(\tilde{r},k_z\right)+\frac{1}{\tilde{r}}\frac{\partial}{\partial\tilde{r}}\tilde{\varphi}_{out}\left(\tilde{r},k_z\right)-\tilde{\varphi}_{out}\left(\tilde{r},k_z\right)=0, \tag{A18}$$

which has solutions of the form:

$$\tilde{\varphi}_{out}\left(\tilde{r},k_z\right)=d_1\left(k_z\right)I_0\left(\tilde{r}\right)+d_2\left(k_z\right)K_0\left(\tilde{r}\right). \tag{A19}$$

Applying the boundary condition, eq. (A8), leads to

$$d_2\left(k_z\right)=-d_1\left(k_z\right)\frac{I_0\left(k_zb\right)}{K_0\left(k_zb\right)}, \tag{A20}$$

and hence eq. (A19) becomes

$$\tilde{\varphi}_{out}\left(\tilde{r},k_z\right)=d_1\left(k_z\right)\left[I_0\left(\tilde{r}\right)-\frac{I_0\left(k_zb\right)}{K_0\left(k_zb\right)}K_0\left(\tilde{r}\right)\right]. \tag{A21}$$

The two remaining coefficients, $c_1\left(k_z\right)$ and $d_1\left(k_z\right)$, are determined by the conditions at the beam boundary, $r=R$, which read

$$\tilde{\varphi}_{out}\left(k_zR,k_z\right)=\tilde{\varphi}_{in}\left(k_zR,k_z\right), \tag{A22}$$

and

$$\frac{\partial}{\partial\tilde{r}}\tilde{\varphi}_{out}\left(\tilde{r},k_z\right)\Big|_{\tilde{r}=k_zR;\ k_z=const.}=\frac{\partial}{\partial\tilde{r}}\tilde{\varphi}_{in}\left(\tilde{r},k_z\right)\Big|_{\tilde{r}=k_zR;\ k_z=const.}. \tag{A23}$$

Eqs. (A22) and (A23) produce

$$d_1\left(k_z\right)=-\frac{Q_e}{\varepsilon_0\pi k_zR^2}\frac{RI_1\left(k_zR\right)K_0\left(k_zb\right)}{I_0\left(k_zb\right)}e^{-\frac{k_z^2\sigma_z^2}{2}}, \tag{A24}$$

and

$$c_1\left(k_z\right)=-\frac{Q_e}{\varepsilon_0\pi k_zR}e^{-\frac{k_z^2\sigma_z^2}{2}}\left[I_1\left(k_zR\right)\frac{K_0\left(k_zb\right)}{I_0\left(k_zb\right)}+K_1\left(k_zR\right)\right], \tag{A25}$$

where we used relations

$$\frac{d}{dz}K_0\left(z\right)=-K_1\left(z\right), \tag{A26}$$

and

$$\frac{d}{dz}I_0\left(z\right)=I_1\left(z\right), \tag{A27}$$

and

$$I_\nu\left(z\right)K_{\nu+1}\left(z\right)+I_{\nu+1}\left(z\right)K_\nu\left(z\right)=\frac{1}{z}. \tag{A28}$$

Inserting eqs. (A24) and (A25) into eqs. (A21) and (A17) generates

$$\tilde{\varphi}_{in}\left(r,k_z\right)=-\frac{Q_e}{\varepsilon_0\pi R^2}e^{-\frac{k_z^2\sigma_z^2}{2}}\left\{\frac{R}{k_z}\left[\frac{I_1\left(k_zR\right)K_0\left(k_zb\right)+K_1\left(k_zR\right)I_0\left(k_zb\right)}{I_0\left(k_zb\right)}\right]I_0\left(k_zr\right)-\frac{1}{k_z^2}\right\}, \tag{A29}$$

for $r \le R$ and

$$\tilde{\varphi}_{out}\left(r,k_z\right) = -\frac{Q_e R}{\varepsilon_0 \pi k_z R^2} e^{-\frac{k_z^2\sigma_z^2}{2}} \frac{I_1\left(k_z R\right)}{I_0\left(k_z b\right)} \left[K_0\left(k_z b\right) I_0\left(k_z r\right) - I_0\left(k_z b\right) K_0\left(k_z r\right) \right], \tag{A30}$$

for $R < r \le b$.

The electric potential inside the bunch is given by the inverse Fourier transformation of eq. (A29), i.e.

$$\varphi_{in}\left(r,z\right) = \frac{1}{2\pi} \int_{-\infty}^{\infty} \tilde{\varphi}_{in}\left(r,k_z\right) e^{ik_z z}\, dk_z \ , \tag{A31}$$

which leads to the longitudinal electric field:

$$E_{z,in}\left(r,z\right) = -\frac{\partial}{\partial z}\varphi_{in}\left(r,z\right) = -\frac{i}{2\pi} \int_{-\infty}^{\infty} k_z \tilde{\varphi}_{in}\left(r,k_z\right) e^{ik_z z}\, dk_z \ . \tag{A32}$$

On the bunch axis, $r = 0$ and the longitudinal electric field is

$$\begin{aligned} E_{z,in}\left(0,z\right) &= -\frac{i}{2\pi} \int_{-\infty}^{\infty} k_z \tilde{\varphi}_{in}\left(0,k_z\right) e^{ik_z z}\, dk_z \\ &= \frac{Q_e}{\varepsilon_0 \pi R} \frac{i}{2\pi} \int_{-\infty}^{\infty} e^{-\frac{k_z^2\sigma_z^2}{2}} \left\{ \frac{I_1\left(k_z R\right) K_0\left(k_z b\right)}{I_0\left(k_z b\right)} + K_1\left(k_z R\right) - \frac{1}{k_z R} \right\} e^{ik_z z}\, dk_z \ , \\ &= \frac{Q_e}{\varepsilon_0 \pi R} \frac{i}{2\pi} \int_0^{\infty} \left[f\left(k_z\right) e^{ik_z z} + f\left(-k_z\right) e^{-ik_z z} \right] dk_z \end{aligned} \tag{A33}$$

with

$$f\left(k_z\right) = e^{-\frac{k_z^2\sigma_z^2}{2}} \left\{ \frac{I_1\left(k_z R\right) K_0\left(k_z b\right) + I_0\left(k_z b\right) K_1\left(k_z R\right)}{I_0\left(k_z b\right)} - \frac{1}{k_z R} \right\} . \tag{A34}$$

The function, $f\left(k_z\right)$, is an odd function of k_z. To prove it, it is sufficient to show that the function,

$$h\left(k_z\right) = I_1\left(k_z R\right) K_0\left(k_z b\right) + I_0\left(k_z b\right) K_1\left(k_z R\right) \tag{A35}$$

is odd, or more explicitly,

$$h\left(k_z\right) + h\left(-k_z\right) = I_1\left(k_z R\right) \left[K_0\left(k_z b\right) - K_0\left(-k_z b\right) \right] + I_0\left(k_z b\right) \left[K_1\left(k_z R\right) + K_1\left(-k_z R\right) \right], \tag{A36}$$

vanishes for any real value of k_z. The integral representations of the modified Bessel function of the 0^{th} order read

$$K_0\left(z\right) = -\frac{1}{\pi} \int_0^{\pi} e^{\pm z\cos\theta} \left[\gamma + \ln\left(2z\sin^2\theta\right) \right] d\theta, \tag{A37}$$

and

$$I_0\left(z\right) = \frac{1}{\pi} \int_0^{\pi} e^{\pm z\cos\theta}\, d\theta \ , \tag{A38}$$

where

$$\gamma \equiv \lim_{n\to\infty} \left(1 + \frac{1}{2} + \frac{1}{3} + \cdots + \frac{1}{n} - \ln n \right) \approx 0.5772156649... \tag{A39}$$

is the Euler's constant. It follows from eq. (A37) that

$$K_0(z)-K_0(-z)=-\frac{1}{\pi}\int_0^{\pi}e^{\pm z\cos\theta}\left[\ln\left(2z\sin^2\theta\right)-\ln\left(-2z\sin^2\theta\right)\right]d\theta$$
$$=\frac{\ln(-1)}{\pi}\int_0^{\pi}e^{\pm z\cos\theta}\,d\theta \quad , \quad \text{(A40)}$$
$$=i\pi(2n+1)I_0(z)$$

with n being an arbitrary integer. Taking the first derivative of eq. (A40) gives

$$K_1(z)+K_1(-z)=-i\pi(2n+1)I_1(z). \quad \text{(A41)}$$

Making use of eqs. (A40) and (A41), eq. (A36) becomes

$$h(k_z)+h(-k_z)=i\pi(2n+1)I_1(k_zR)I_0(k_zb)-i\pi(2n+1)I_1(k_zR)I_0(k_zb)=0, \quad \text{(A42)}$$

and consequently we proved that $f(k_z)$ is an odd function, i.e.

$$f(-k_z)=-f(k_z). \quad \text{(A43)}$$

Inserting eq. (A43) into eq. (A33), we obtain

$$E_{z,in}(0,z)=-\frac{Q_e}{\varepsilon_0\pi^2R}\int_0^{\infty}f(k_z)\sin(k_zz)dk_z$$
$$=-\frac{Q_e}{\varepsilon_0\pi^2R}\int_0^{\infty}e^{-\frac{k_z^2\sigma_z^2}{2}}\left\{\frac{I_1(k_zR)K_0(k_zb)}{I_0(k_zb)}+K_1(k_zR)-\frac{1}{k_zR}\right\}\sin(k_zz)dk_z \quad . \quad \text{(A44)}$$

It is often convenient to express eq. (A44) in terms of the normalized variables

$$E_{z,in}(0,\bar{z})=-\frac{Q_e}{\varepsilon_0\pi^2\bar{R}\sigma_z^2}\int_0^{\infty}e^{-\frac{\xi^2}{2}}\left\{\frac{I_1(\xi\cdot\bar{R})K_0(\xi\cdot\bar{b})}{I_0(\xi\cdot\bar{b})}+K_1(\xi\cdot\bar{R})-\frac{1}{\xi\bar{R}}\right\}\sin(\xi\cdot\bar{z})d\xi, \quad \text{(A45)}$$

with $\bar{R}=R/\sigma_z$, $\bar{z}=z/\sigma_z$ and $\bar{b}=b/\sigma_z$. Applying the asymptotic behavior of the modified Bessel function at $k_z\to 0$ yields

$$\lim_{k_z\to 0}\left[f(k_z)\sin(k_zz)\right]=\lim_{k_z\to 0}\left\{\left[-\frac{k_zR}{2}\ln(k_zb)+\frac{1}{k_zR}-\frac{1}{k_zR}\right]\sin(k_zz)\right\}=0. \quad \text{(A46)}$$

At $k_z\to\infty$, the asymptotic behaviors of the modified Bessel functions are

$$I_{0,1}(x) \quad \frac{e^x}{\sqrt{2\pi x}},$$
$$K_{0,1}(x) \quad \sqrt{\frac{\pi}{2x}}e^{-x},$$

and hence it follows

$$\lim_{k_z\to\infty}\left[f(k_z)\sin(k_zz)\right]=\lim_{k_z\to\infty}\left\{e^{-\frac{k_z^2\sigma_z^2}{2}}\left(\sqrt{\frac{\pi}{2k_zR}}e^{-k_z(2b-R)}+\sqrt{\frac{\pi}{2k_zR}}e^{-k_zR}-\frac{1}{k_zR}\right)\sin(k_zz)\right\}$$
$$=0 \quad . \quad \text{(A47)}$$

Eqs. (A46) and (A47) suggest that the integrand of integral in eq. (A44), is a finite real function. Fig. A1 compares the results in eq. (A44) with the previously derived longitudinal space charge field in the absence of the beam pipe and with the longitudinal

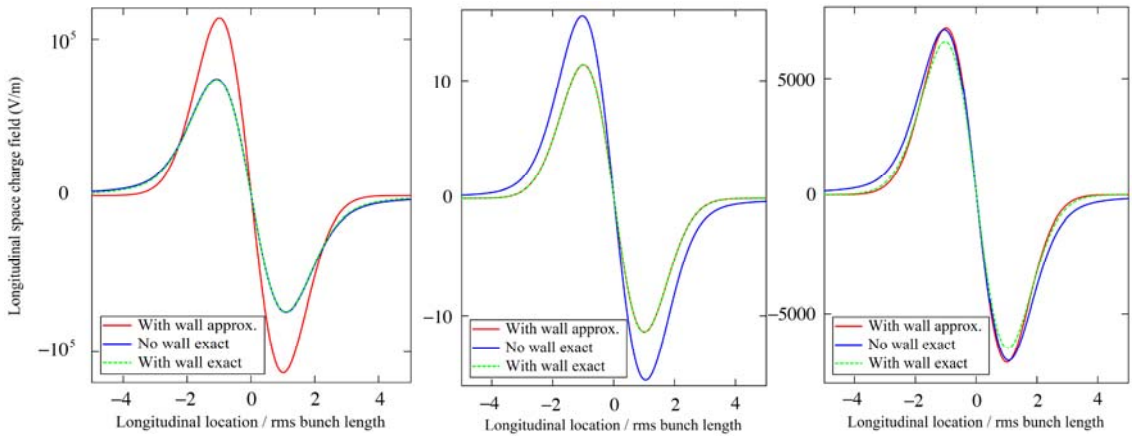

(a) (b) (c)

Figure A1: the exact longitudinal space charge field in the presence of the beam pipe with 5 cm radius. The abscissas are the longitudinal location in unit of R.M.S. bunch length and the ordinates are the longitudinal space charge field in unit of V/m. The green dash curve shows the field calculated from the exact solution, i.e. eq. (A44), the blue solid curve shows the field from the electron bunch, without beam pipe being considered, and the red solid curve shows the field calculated from an approximate formula where shielding from the beam pipe is considered but the electron bunch is assumed to be much longer than the beam pipe radius. (a) calculated for PoP parameters but with 1.26 cm lab frame rms bunch length; (b) calculated with 1.26 m beam frame rms bunch length; (c) calculated with 5 cm beam frame rms bunch length.

space charge field in the presence of the beam pipe but with long beam approximation. As shown in Fig. A1(a), when the beam frame bunch length, 1.26 cm is much smaller than the 5cm beam pipe radius, the exact solution (green) in eq. (28) overlaps with that for an open beam (blue), i.e. without beam pipe. Fig. A1(b) shows that as the beam frame bunch length increases to 1.26 m, the exact solution overlaps with that of the long bunch approximation (red). With the R.M.S. bunch length of 5cm, Fig. A1(c) shows that the exact solution deviates from both of the other solutions.